REPORT NO. RD-TM-68-2

AN EXPERIMENTAL INVESTIGATION OF DOWNSTREAM FLOW-FIELD PROPERTIES BEHIND A FORWARD LOCATED SONIC JET INJECTED INTO TRANSONIC FREESTREAM FROM A BODY OF REVOLUTION

by

C. W. Duhlke

January 1968

U.S. ARMY MISSILE COMMAND
Redstone Arsenal, Alabama

2 January 1968

Report No. RD-TM-68-2

AN EXPERIMENTAL INVESTIGATION OF DOWNSTREAM FLOW-FIELD PROPERTIES BEHIND A FORWARD LOCATED SONIC JET INJECTED INTO TRANSONIC FREESTREAM FROM A BODY OF REVOLUTION

by

C. W. Dahlke

DA Project No. 1T012001A91A
AMC Management Structure Code No. 5016.11.8400

Aerodynamics Branch
Advanced Systems Laboratory
Research and Development Directorate
U. S. Army Missile Command
Redstone Arsenal, Alabama 35809

ABSTRACT

Transonic wind-tunnel investigation was conducted to determine the nature of the flow field downstream of a lateral sonic jet on a body of revolution. The survey was made in a plane normal to the body centerline 9.25 body diameters aft of the lateral jet nozzle. Velocity measurements were made by a remotely driven Pitot-static probe at wind-tunnel Mach numbers of 0.9 and 1.2. The data are presented in the form of Mach number vectors mapped in the normal plane for three pressure ratios and for model angles of attack of 0.0 and 1.0 deg.

Results indicate a pair of trailing vortices in the jet wake on opposite sides of the jet centerline. The strength and position appear to be strong functions of pressure ratios and freestream Mach number. These data indicate a method for developing means of determining aerodynamic forces on stabilizing surfaces for missiles with forward jets.

CONTENTS

ILLUSTRATIONS

SYMBOLS

a	Speed of sound (~ ft/sec)
D	Model diameter (5.5 in.)
d_j	Jet exit diameter
f	Vortex center outboard coordinate (in.)
h	Vortex center vertical coordinate (in.)
ℓ	Distance from jet centerline to probe station
M	Mach number
M_X, M_Y, M_Z	Components of Mach number along X, Y, Z cocrdinates, respectively
P	Pressure
$P_1 - P_6$	Probe pressures
R	Body radius (2.75 in.)
V	Velocity
X, Y, Z	Rectangular coordinates, X, along model centerline with origin at nose apex
α	Angle of attack pitch plane (deg)
Γ	Vorticity or vortex strength (~ ft^2/sec)
ψ	Angle of attack, yaw plane (deg)

Subscripts

c	Plenum chamber
i	Image vortex
j	Jet conditions

SYMBOLS (Concluded)

ℓ	Vortex (lower) below jet centerline
p	Probe measured parameter
u	Vortex (upper) above jet centerline
∞	Freestream condition

1. Introduction

Currently, the missile aerodynamicist is confronted more and more with the problem of assessing the flow interaction interference produced by injecting a secondary gas stream into the primary flow field. Such cases occur when reaction jets are used for control, to provide a spin impulse, or where residual gases from pressurization systems and similar devices are expelled. When these gases are injected near the nose of the missile body, it has been observed that large changes occur in the stability, control, and rolling moment characteristics. This effect has been attributed largely to the resulting changes in the flow field over the fin stabilizing surfaces.

Previous analytical and experimental research studies have concentrated on the flow-field interaction in the vicinity of the secondary jet exit. Most of the studies have considered the two-dimensional problem with a supersonic primary flow. Little has been accomplished in determining the flow-field properties induced by the jet at large distances downstream of the injection point.

The present study was undertaken to provide some insight into the details of the perturbed flow field which was observed to produce large changes in the aerodynamic loads of missile stabilizing surfaces. The detailed flow-field structure was measured by a six-tube yaw head pressure probe which was calibrated to give the local Mach number, dynamic pressure, and the pitch and yaw angles of the local velocity vector. The basic model configuration was a body of revolution with a four-caliber ogive nose and a cylindrical afterbody. A single circular sonic nozzle was located three body diameters from the body apex with its axis normal to the body centerline and oriented radially in the yaw plane. The flow field was surveyed in a plane normal to the body centerline 9.25 body diameters aft of the lateral jet nozzle. Measurements were made in the Cornell Aeronautical Laboratory (CAL) 8-ft transonic wind tunnel at freestream Mach numbers of 0.9 and 1.2, angles of attack of 0 and 1 deg, and jet chamber to freestream static pressure ratios of 0, 20, and 80.

The basic results are presented in the form of graphs mapping the Mach number in a plane normal to the body's longitudinal axis. The qualitative effects of freestream Mach number, jet pressure ratio, and angle of attack are illustrated in these plots.

2. Apparatus

The test was conducted in CAL's 8-ft transonic wind tunnel. The test setup consisted of a model (body of revolution) mounted on a sting, and a movable Pitot-static probe was mounted on the tunnel strut such that flow-field points around the vicinity of the aft end of the model could be measured.

The model had a four-caliber tangent ogive nose with a 9.89-caliber afterbody. The cylinder diameter was 5.5 in. A lateral jet was located at three calibers from the nose apex. The nozzle was circular with a sonic exit of 0.44 in. in diameter. Model attitude was maintained by a bubble for angles of attack of 0 and +1 deg. The model was suspended from the sting by a five-component strain gage balance which had been previously designed and built by CAL for U. S. Army Missile Command (AMC), Redstone Arsenal, Alabama. The balance measurements were not required for this test; however, this phase of the test was one of a three-phase test in which the other two phases required use of the balance. The balance outputs for normal force and pitching moment were used to set the model at -1 deg angle of attack for a portion of this phase, and all balance outputs were recorded throughout the test. A total pressure orifice and a thermocouple were installed in the jet plenum chamber.

The flow-angle probe was supplied by CAL (Figure 1). This probe has a hemispherical head $^{3}/_{16}$ in. in diameter. The hemisphere has pressure orifices located at the center and 45 deg each side of the center in both pitch and yaw planes. A ring of static pressure orifices connected to a common manifold on the cylindrical part of the probe was located 10 diameters behind the head. All pressures were routed to a scanivalve on the probe support.

Figures 2 through 4 show the model and probe installed together in the 8-ft test section. The probe forward end was 12.05 body diameter aft of the nose apex. The lateral probe position was achieved by rotation within the probe mount, and the vertical position by translation of the model and sting on the tunnel strut. A smaller roll mechanism was used to level the forward probe orifices at each of the lateral probe positions.

The geometric angles were estimated by CAL to be accurate to ±0.02 deg. The probe local flow angles, as deduced from the probe calibrations, are accurate to ±0.2 deg within the linear range of ±6 deg. The transducer measuring plenum chamber pressure was calibrated to an accuracy of ±1.0 lb/in.^{2}

FIGURE 1. FLOW-ANGLE PROBE

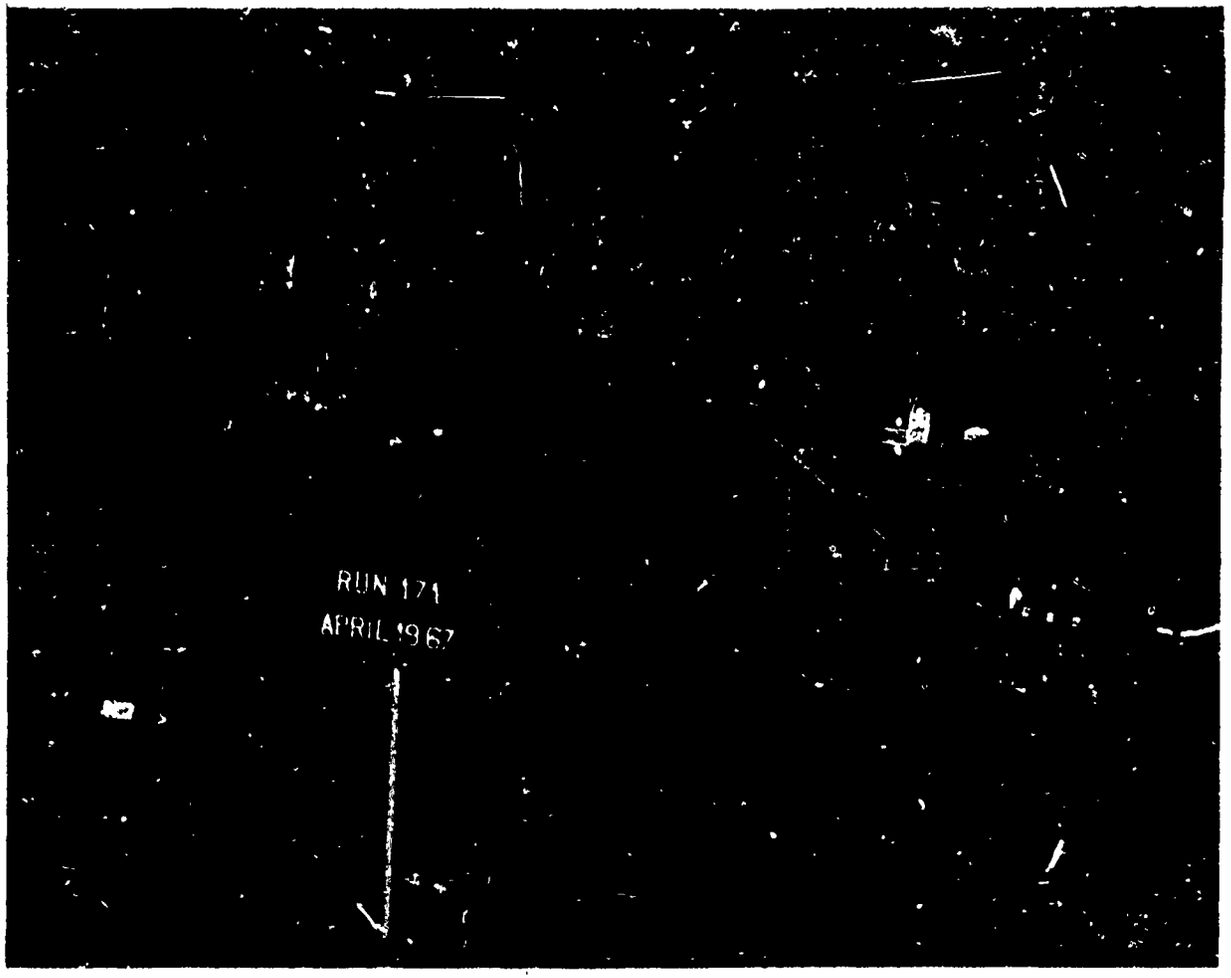

FIGURE 2. MODEL AND PROBE INSTALLED IN THE 8-FOOT TEST SECTION

FIGURE 3. MODEL AND PROBE INSTALLED IN THE 8-FOOT TEST SECTION

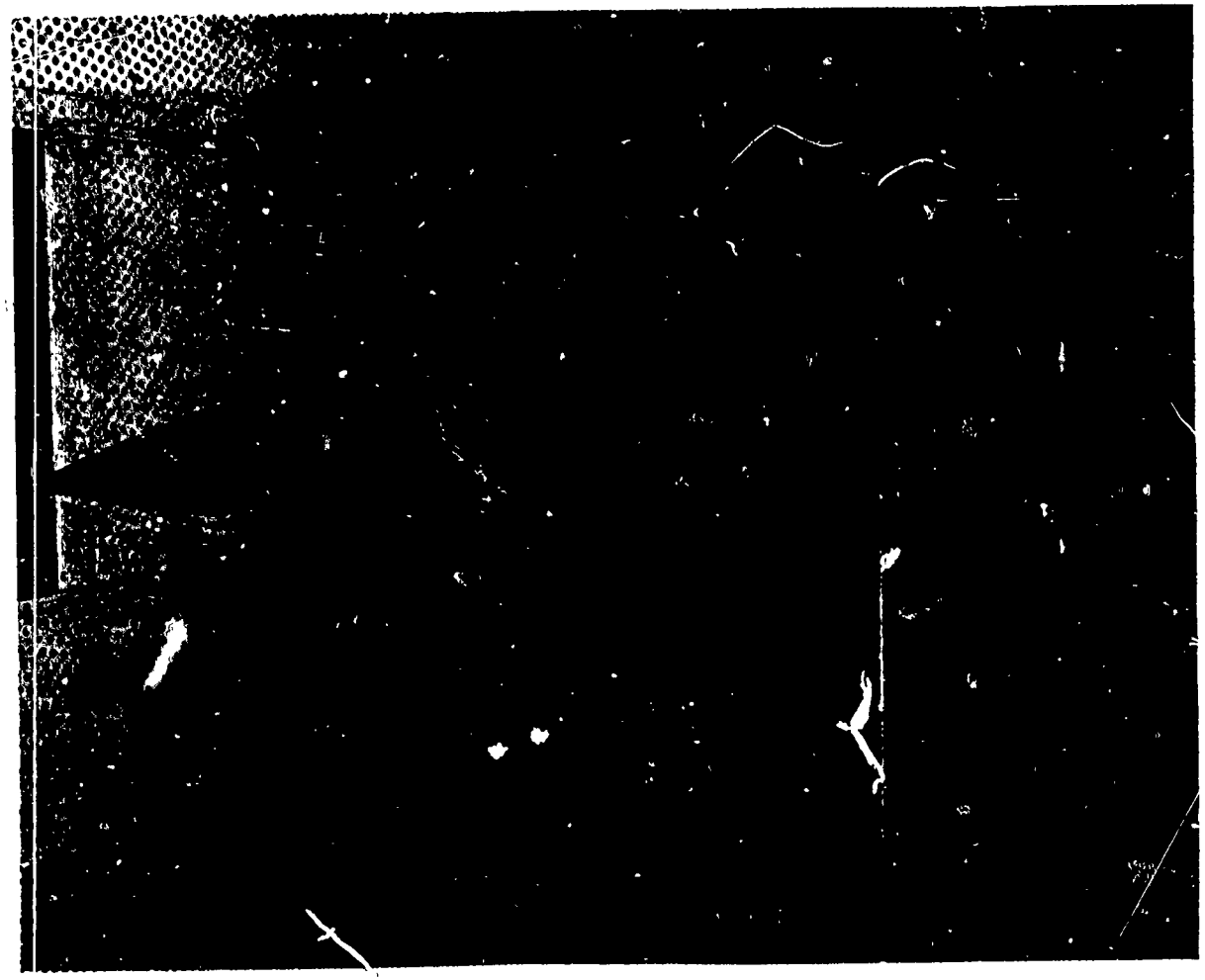

FIGURE 4. MODEL AND PROBE INSTALLED IN THE 8-FOOT TEST SECTION

3. Procedures

The test was conducted at tunnel freestream Mach numbers of 0.9 and 1.2. These were the two Mach numbers for which CAL had calibrated the flow-angle probe. Flow-field surveys at these two Mach numbers were conducted at model plenum chamber pressure to tunnel freestream static pressure ratios of 0 (jet off), 20, and 80. The probe was always aligned parallel to the tunnel centerline. The survey was conducted over a plane always normal to the model centerline. This plane is defined by rectangular coordinates Y, Z with the origin being on the model centerline at 12.05 model diameters (calibers) from the nose apex. The lateral coordinate Y was obtained by a remote roll mechanism allowing the probe to be moved away from the model in an arc, and the vertical coordinate Z was obtained by vertical translation of the model and sting on the tunnel strut. This way displacement was achieved both horizontally and vertically. One run usually consisted of fixing Mach number, model angle of attack, P_c/P_∞, and the lateral position Y while the model was translated vertically with predetermined stops Z to take data. This Z sweep was usually repeated until all three pressure ratios of 0, 20, and 80 were measured for all Z on a fixed Y coordinate. Local Mach number was computed by:

$$M_p = \left[5 \left(\frac{P_5}{P_6} \right)^{2/7} - 5 \right]^{1/2},$$

where P_5 was the measured stagnation pressure (center orifice), and P_6 was measured static pressure. Angles in the pitch α_p and yaw ψ_p direction were determined by comparing differential pressures on the orifices 45 deg around spherical nose $P_2 - P_1$ (pitch) and $P_4 - P_3$ (yaw) to the previously calibrated differential pressure as a function of pitch and yaw angles. The data output consisted of tunnel conditions, model plenum chamber (nitrogen) condition, geometric setup (i.e., α, Y, Z), and the probe outputs with computed M_p, α_p, and ψ_p.

4. Discussion

The data reduction by CAL included a computation of the local Mach number M_p measured by the probe and angles in pitch α_p and yaw ψ_p determined from probe differential pressure measurements[1] and previous calibrations. The survey coordinates were taken in the rectangular coordinate system with

the origin being the model centerline at X = 12.05 calibers from the nose apex. Figure 5 shows a geometric representation of the flow angularity in the X, Y, Z coordinate system. The longitudinal X, lateral Y, and vertical Z Mach number components are computed with the following relations, respectively:

$$M_X = M_p \cos \psi_p \cos \alpha_p$$

$$M_Y = M_p \sin \psi_p \cos \alpha_p$$

$$M_Z = M_p \cos \psi_p \sin \alpha_p \ .$$

The pitch angle α_p used in these equations consists of the probe measured pitch angle plus the model geometric angle of attack. The sign convention specifies that from an aft view positive vectors are to the right and up in the Y, Z plane, and this represents the postive coordinates.

From the onset of the test planning until this presentation of the test analysis the object of this flow-field survey was an attempt to explore the downstream jet effects and to determine what phenomena of jet gas and free-stream interaction induce forces on missile stabilizing surfaces. These data are arranged to give a graphical view of what flow-field perturbation may exist downstream of a lateral jet on a body of revolution. Because of the exploratory nature of this test, and since there are no methods that satisfactorily predict the jet-core position at large distances downstream of the jet, the region over which the survey was conducted was arbitrary. One guide that was available was the loads shown on fins from force test. The forces on horizontal fins with forward located jets[2-5] have shown significant changes in fin loads due to angle of attack, and large induced aerodynamic rolling moments when the forward jets are canted to give missile spin torque have been shown.[2,3]

Based on this experience the survey was designed to explore the region in which most missile type stabilizing surfaces would be within, and as far beyond this region as the equipment physical limitations and time would allow. Increments along both Y and Z coordinates were chosen to be usually 0.5 in. The angle of attack of 1.0 deg was chosen because previous force data had shown significant nonlinear effects there, or at 1.0 deg the percent change due to the jet was larger than at larger angles of attack. The jet was placed in the lateral (horizontal along Y axis) plane because previous tests on the LANCE missile with two opposed forward straight-out vents[3] had shown largest effects on stability when the missile was in a roll position with vents in the lateral plane (perpendicular to the α or wind plane). Even though the test was based

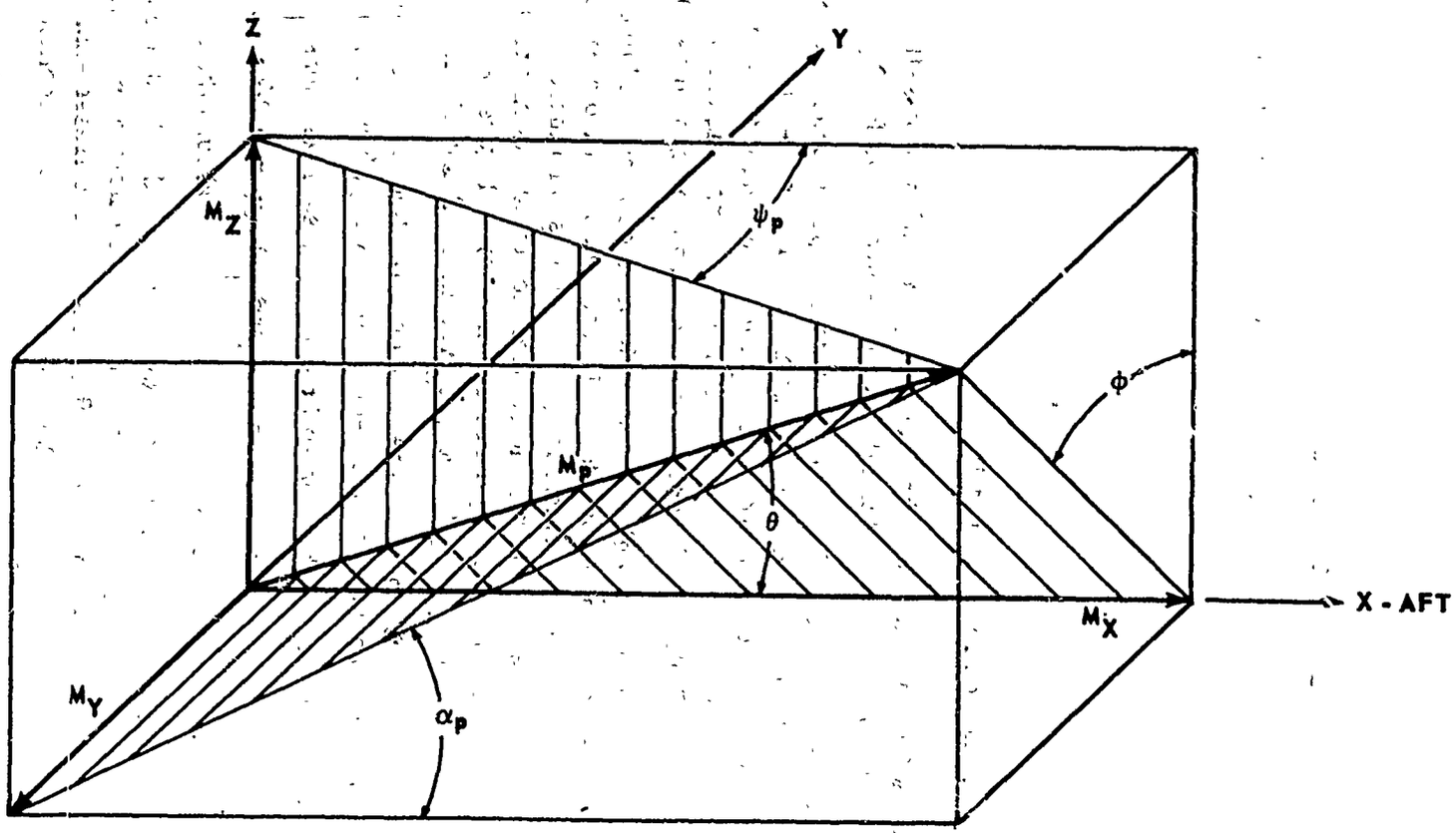

FIGURE 5. MACH NUMBER VECTOR COORDINATE GEOMETRY

somewhat upon past experience, the test and analysis presented herein fulfill the requirement of an exploratory investigation of the flow field downstream of a lateral jet and freestream interaction.

a. Zero Angle-of-Attack Case

The vectors M_{YZ} are presented versus position in the flow field on a scaled grid,

$$\left|M_{YZ}\right| = \sqrt{M_Y^2 + M_Z^2}$$

$$\tan^{-1}\phi = M_Y/M_Z \ ,$$

where M_Y, M_Z, and ϕ are defined in Figure 5.

Figures 6 through 11 show the vector diagrams of the cross-flow pattern for both Mach number 0.9 and 1.2 at all three pressure ratios P_c/P_∞. Figures 6 and 7 show the flow-field pattern at zero angle of attack without jet flow. The survey limits were -8.5 in. along Y axis and from -3.0 to 1.0 in. on the Z axis. Geometric symmetry exists about Z = 0, and it is assumed for zero angle of attack that flow-field symmetry exists on opposing sides of the line Z = 0 in the Y, Z plane. The accuracy for α_p and ψ_p is quoted as ±0.2 deg; however, the repeatability at a given point in the field was observed to be better than ±0.1 deg in either pitch or yaw plane. It should be noted from Figures 6 and 7 that some flow angularity exists for the jet-off case and these angularities are generally within the quoted accuracy of ±0.2 deg, and these are not stripped out of the following data for this report. Figures 8 and 9 show for $M_\infty = 0.9$ and 1.2 at $P_c/P_\infty = 20$ the M_{YZ} versus Y, Z coordinates. Both figures show some velocity in the Z direction along the line Z = 0, and if true symmetry exists this should be a pure Y-direction velocity; however, the α_p angularities are consistant with the jet-off trends. These magnitudes $\left|M_{YZ}\right|$ are scaled to $\left|M_{YZ}\right| = 0.1$/in. at $M_\infty = 0.9$, and $\left|M_{YZ}\right| = 0.2$/in. at $M_\infty = 1.2$. Figure 8 shows a general entrainment of flow around the body from above and below the line Z = 0, with expansion away from the Z = 0 line beyond $Y \cong 7.0$. Figure 9 is the most conclusive plot that was obtained during this survey. Table I presents the momentum flux ratio of jet to freestream for all combinations of M_∞ and P_c/P_∞. It follows from the equation of motion that the

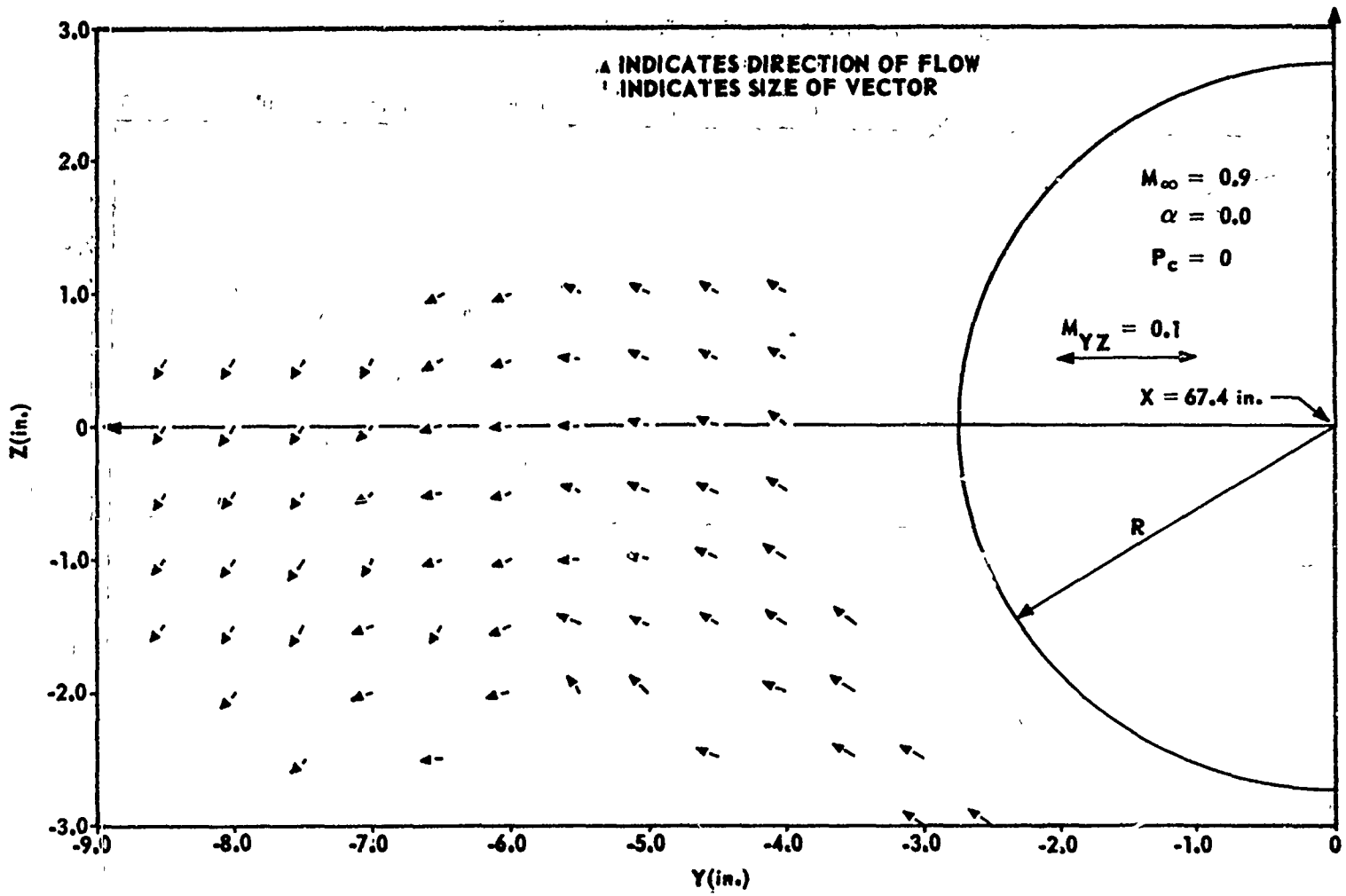

FIGURE 6. FREESTREAM FLOW FIELD

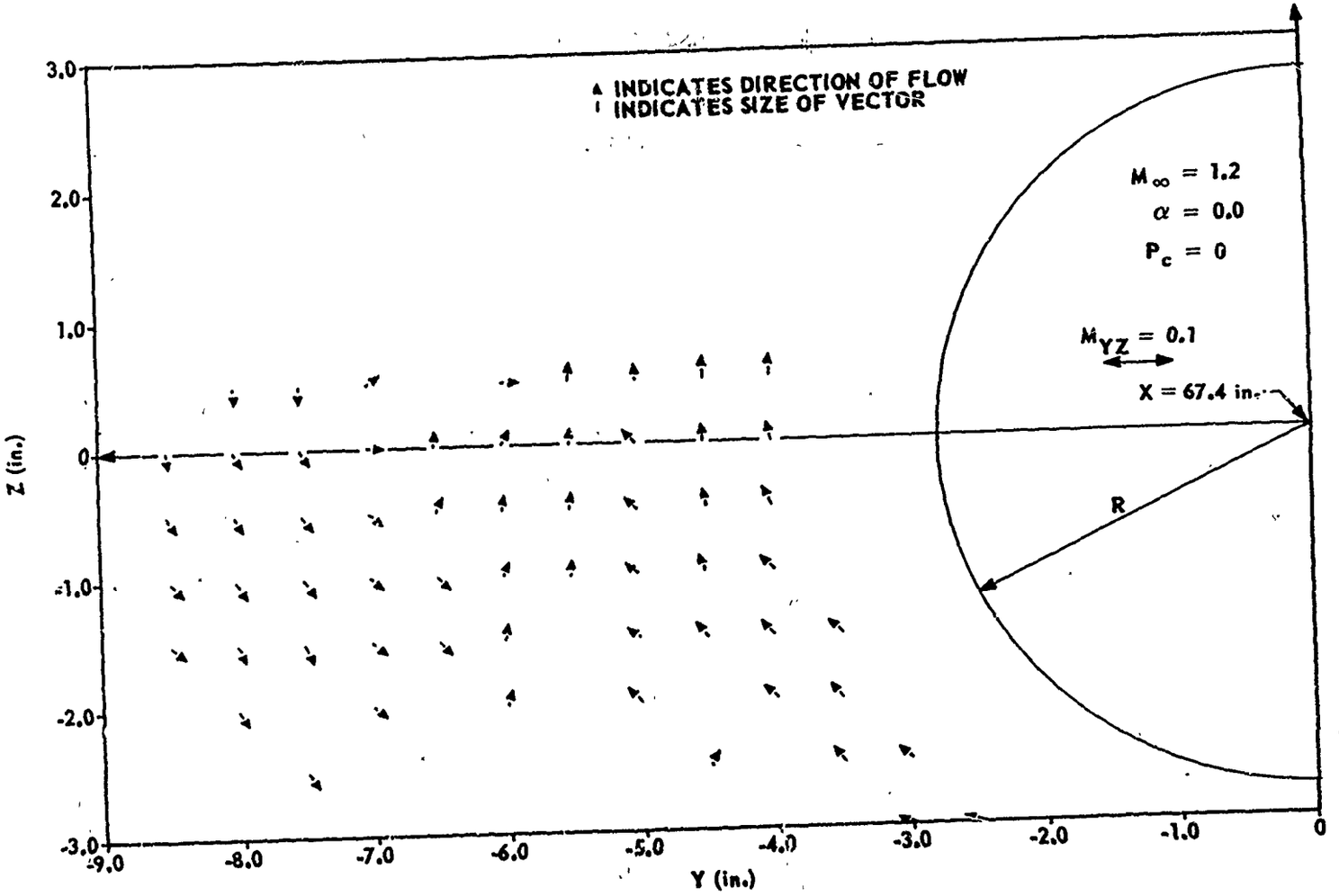

FIGURE 7. FREESTREAM FLOW FIELD

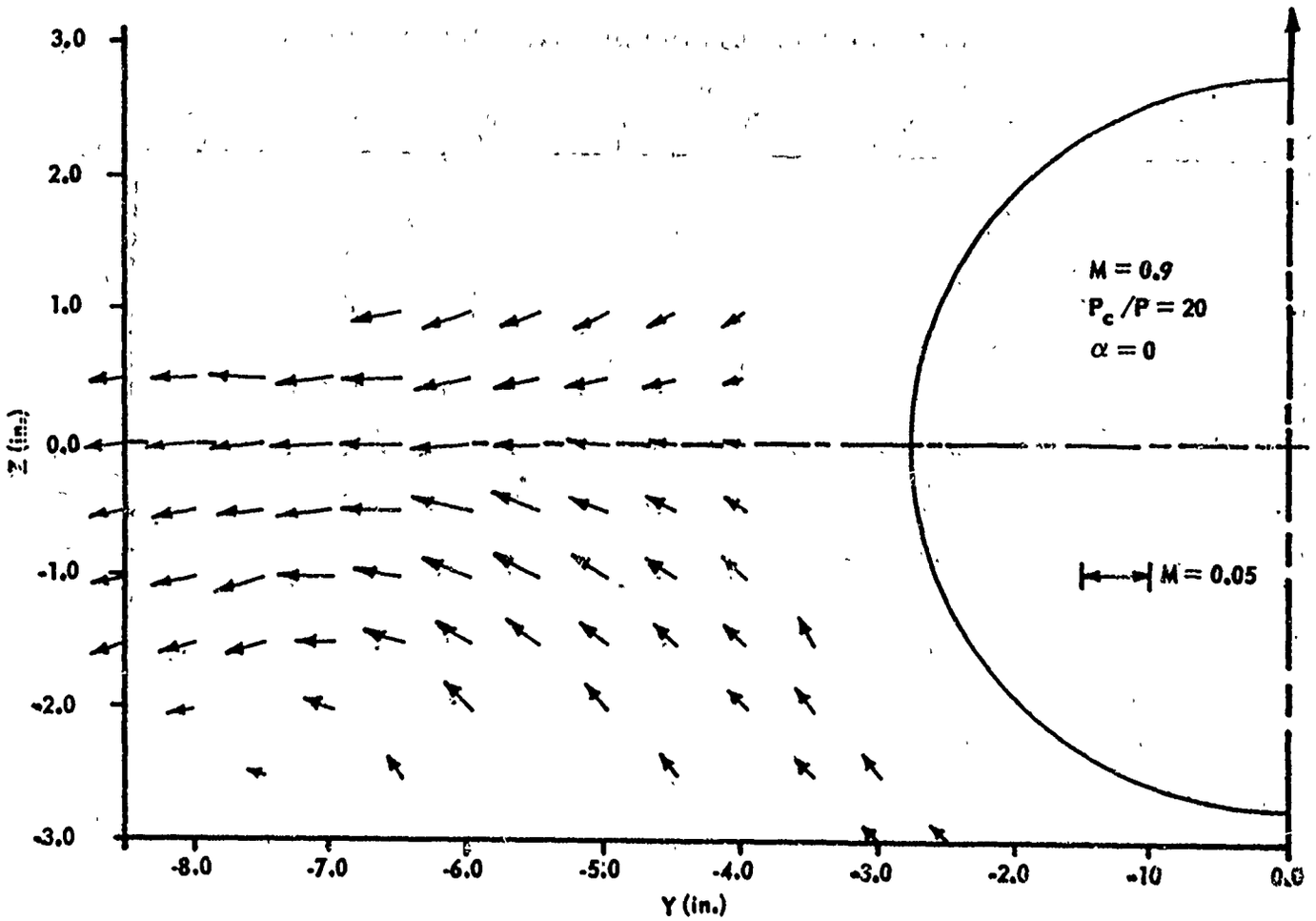

FIGURE 8. JET WAKE IN FREESTREAM FLOW FIELD

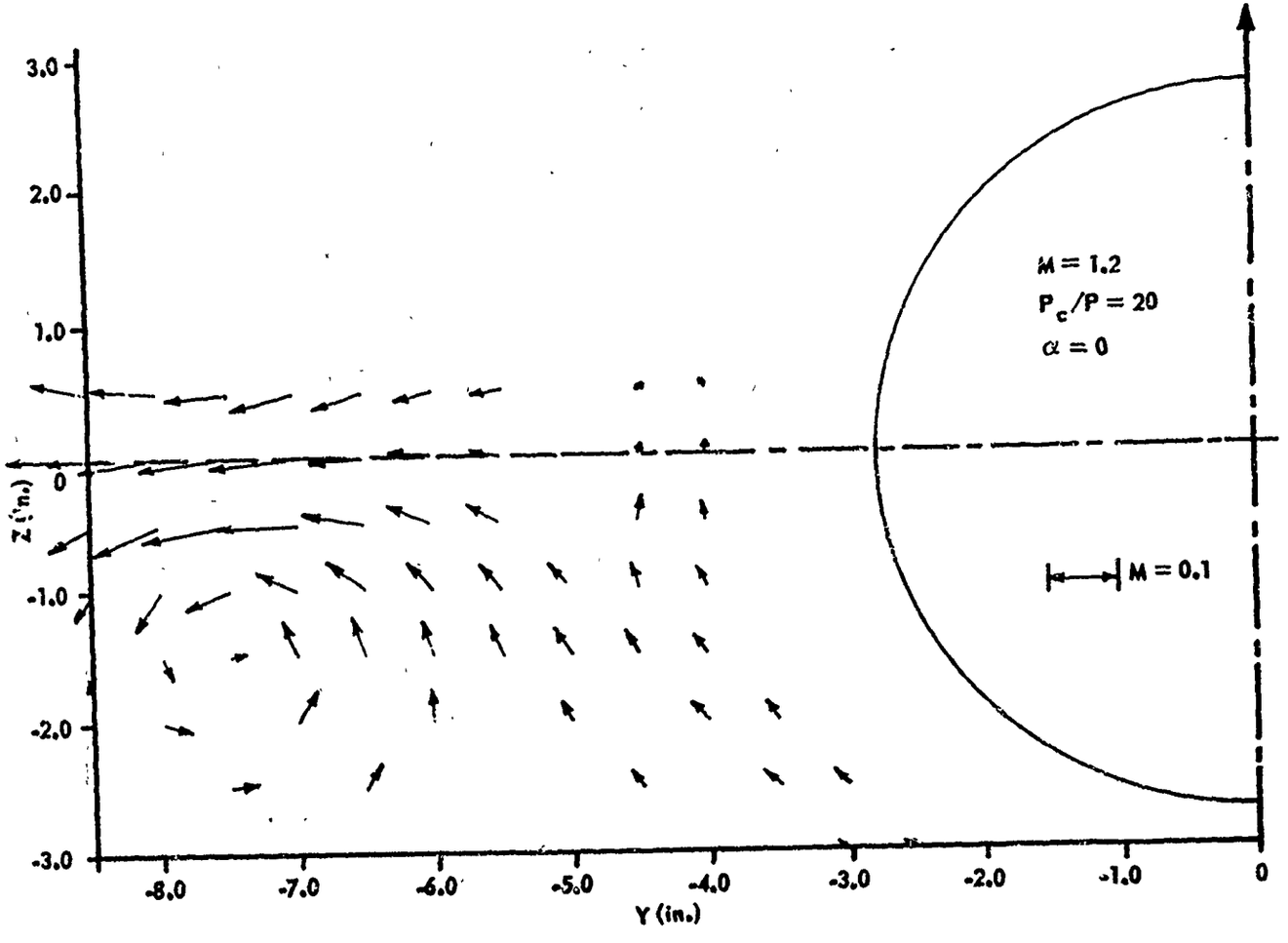

FIGURE 9. JET WAKE IN FREESTREAM FLOW FIELD

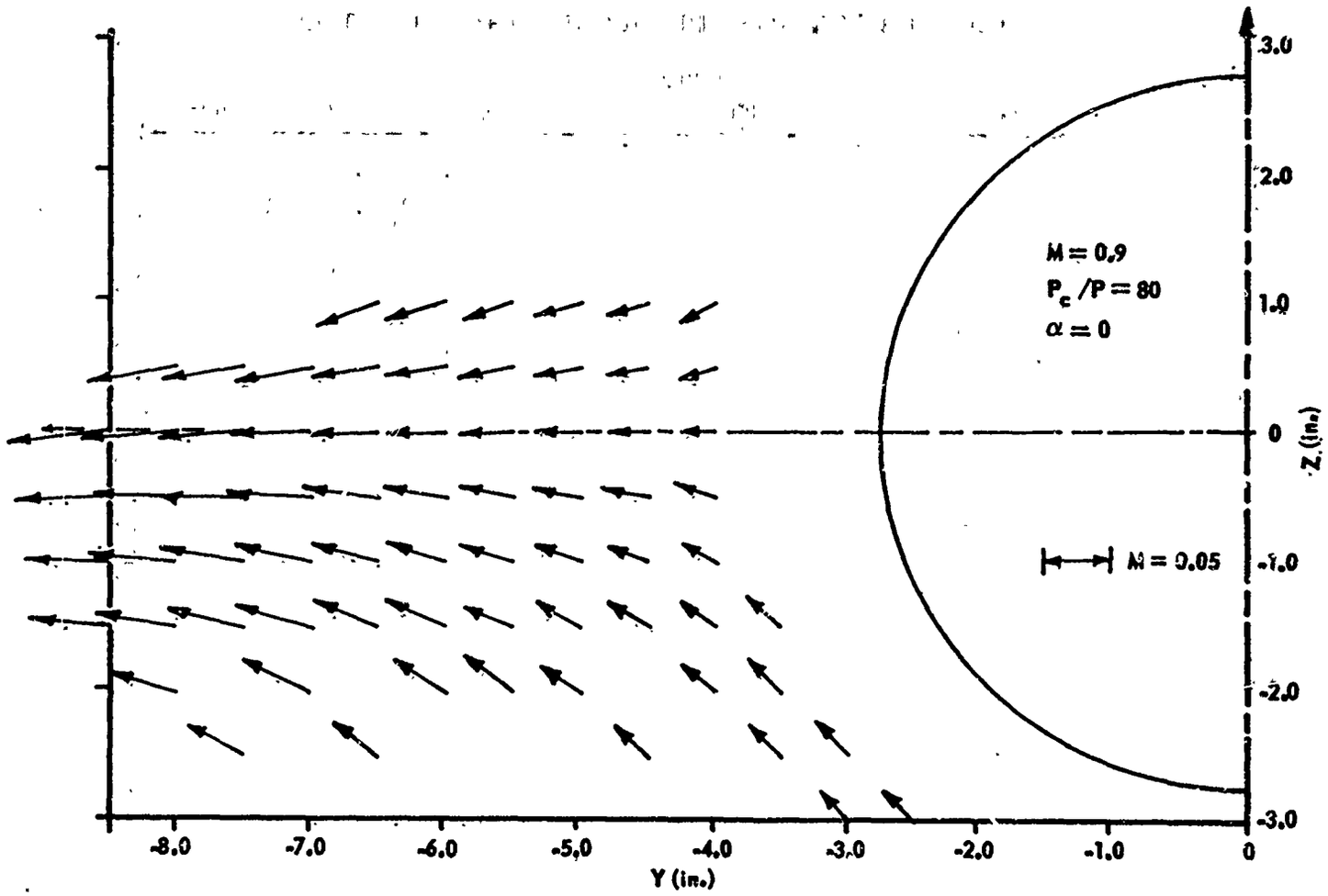

FIGURE 10. JET WAKE IN FREESTREAM FLOW FIELD

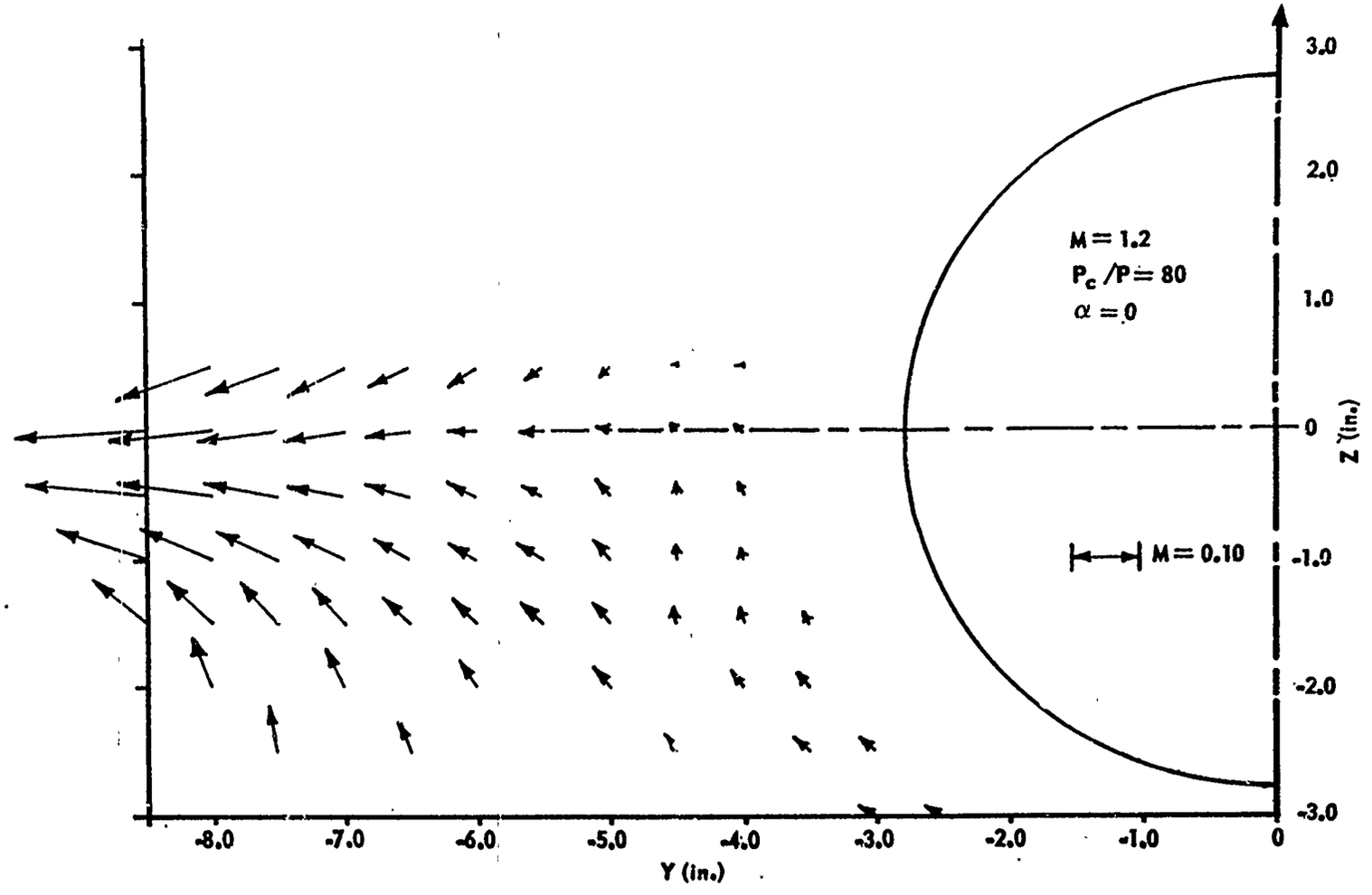

FIGURE 11. JET WAKE IN FREESTREAM FLOW FIELD

higher $\dot{M}_j V_j / \dot{M}_\infty V_\infty$ is, the farther from the exit plane the jet wake is displaced. This figure represents a combination of the highest $M_\infty = 1.2$ and lowest $P_c/P_\infty = 20$ giving the lowest $\dot{M}_j V_j / \dot{M}_\infty V_\infty$ tested. It appears that at this momentum ratio the jet wake for the most part fell within the survey region, or in other words the survey captured the jet-core region for this momentum ratio. Shown here is vortex action deduced to be a cross-sectional view of a trailing vortex in the jet wake, and furthermore if symmetry exists, there will be another vortex with equal vorticity in the upper half of the plane. This then forms a postulation that the downstream jet wake consists of a trailing vortex pair located equidistant from the jet centerline. The existence of a vortex pair for this condition should be typical of all other conditions tested during this survey; then if the survey coordinates had covered a larger region for the conditions shown in Figures 10 and 11, the vortex location would have been apparent. These flow patterns for $P_c/P_\infty = 80$ are similar to the lower pressure patterns, and for $P_c/P_\infty = 80$ at $M_\infty = 1.2$ (Figure 11) it appears the vortex was almost captured. The vortex position and strength estimates for the zero angle-of-attack case are tabulated in Table I. These estimates are based on plane vortex theory using a flow model consisting of twin vortex with boundary conditions of the cylindrical surface.

TABLE I. VORTEX PARAMETERS

P_c/P_∞	$\dot{M}_j V_j / \dot{M}_\infty V_\infty$	f_ℓ (in.)	h_ℓ (in.)	f_u (in.)	h_u (in.)	Γ_ℓ/a^* (ft)
$M_\infty = 0.9$, $\alpha = 0.0$ deg						
20	0.1252	- 7.4	-2.6	-7.4	2.6	0.0300
80	0.5007	- 9.6	-3.6	-9.6	3.6	0.0875
$\alpha = 1.0$ deg						
20	0.1252	- 7.8	-1.72	-6.5	3.48	0.0303
80	0.5007	-10.0	-2.72	-8.7	4.48	0.0875
$M = 1.2$, $\alpha = 0.0$ deg						
20	0.0469	- 7.1	-1.6	-7.1	1.6	0.0629
80	0.1878	- 9.6	-1.7	-9.6	1.7	0.053

*$\Gamma_u = -\Gamma_\ell$

a = local speed of sound

b. One-Degree Angle-of-Attack Case

The model was pitched to 1-deg angle of attack and the same flow-field region was surveyed at $M_\infty = 0.9$ and $P_c/P_\infty = 0$, 20, and 80, however, because of physical limitations of the setup the model was pitched to -1 deg to survey the same region. The $\alpha = -1$-deg case was interpreted to be equivalent to testing the upper half plane at $\alpha = +1$ deg with a change in sign of α_p. This will be true except for small malalignments and differences in set α, but these differences should not effect any general flow-field trends. Figure 12 shows the case for no jet with model at an $\alpha = 1.0$ deg. The row of vectors M_{YZ} along Z = 0 are compared to Beskin's upwash around a body of revolution[6] in Figure 13. Here the zero angle-of-attack case has been subtracted for each point of test. The test results show good agreement with this cross-flow potential solution. Figures 14 and 15 present the two pressure ratios of 20 and 80 for the case of $\alpha = 1.0$ deg at $M_\infty = 0.9$. These plots show a combination of cross flow due to angle of attack and the trailing jet wake vortices. The vortex cores were not captured; however, there appears to be a shift in vortex core location or a twisting effect of the jet wake that may follow the cross-flow streamline pattern for the body at angle of attack. Using this hypothesis the lower vortex would shift up and outboard with respect to the Y axis and the upper vortex would shift up and inboard at $\alpha = 1.0$ deg. Estimates of these vortex core positions, assuming the circulation strength of the pair to be the same as for the $\alpha = 0$ case, were made from plane vortex theory, linearily superimposed on the jet-off angle-of-attack case. These estimates for core location are presented in Table I. The equations used for representing the flow field are based on the hypothesis of the twin vortex pattern shown in Figure 16. The use of plane vortex theory implies that isentropic flow and the velocity perturbation in the X direction are small compared to those in the Y, Z plane. The flow is irrotational everywhere except at the vortex core location which shows up as a singular point in the equations. The equations as used for an iterative determination of vortex core and strength are given as:

$$M_Y = \frac{V_Y}{a} = -\frac{\Gamma}{a}\frac{1}{2\pi}\left[\frac{Z - h_\ell}{(Y - f_\ell)^2 + (Z - h_\ell)^2} - \frac{Z - h_{\ell i}}{(Y - f_{\ell i})^2 + (Z - h_{\ell i})^2}\right.$$

$$\left. - \frac{Z - h_u}{(Y - f_u)^2 + (Z - h_u)^2} + \frac{Z - h_{ui}}{(Y - f_{ui})^2 + (Z - h_{ui})^2}\right]$$

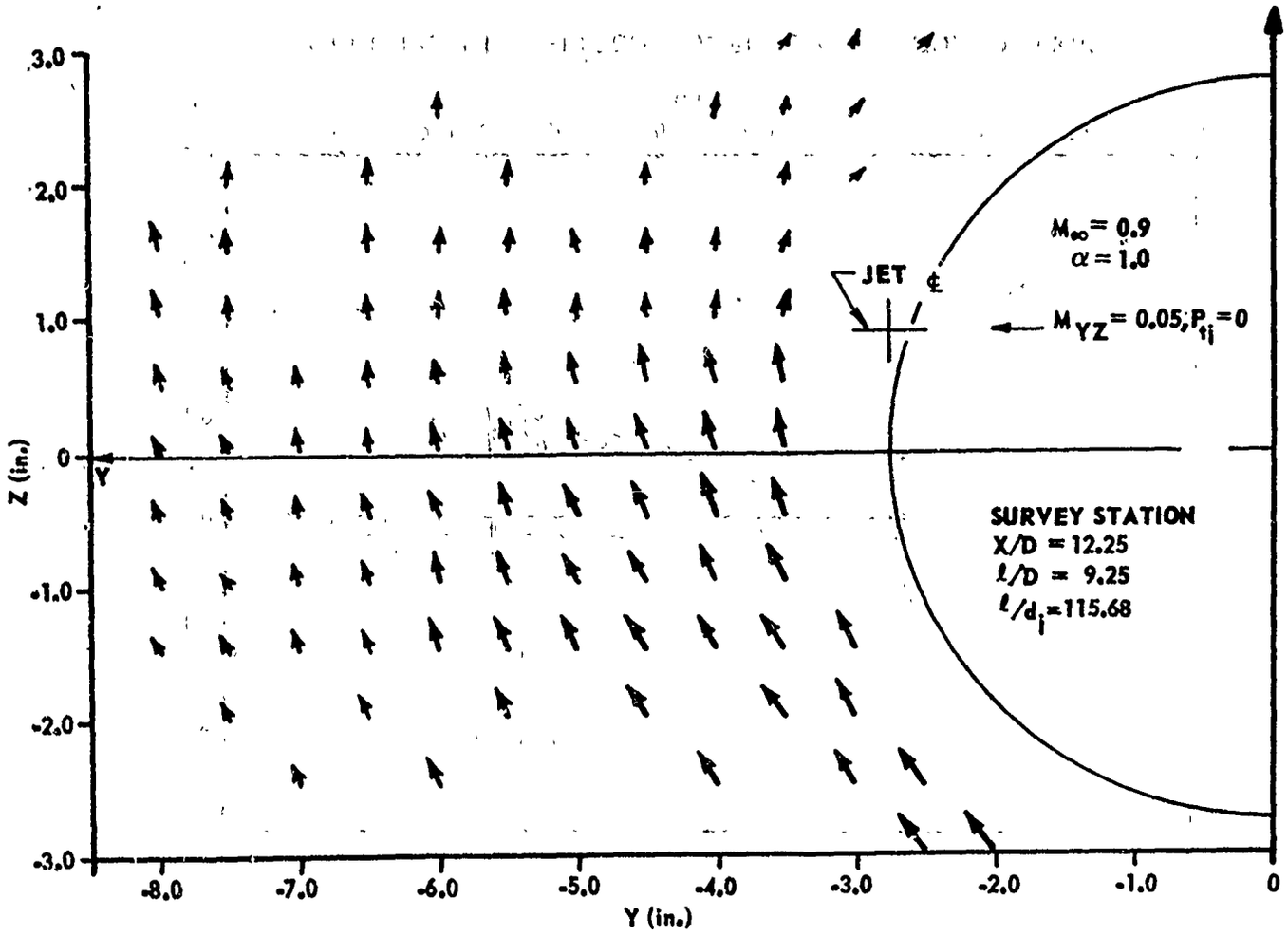

FIGURE 12. FREESTREAM FLOW FIELD

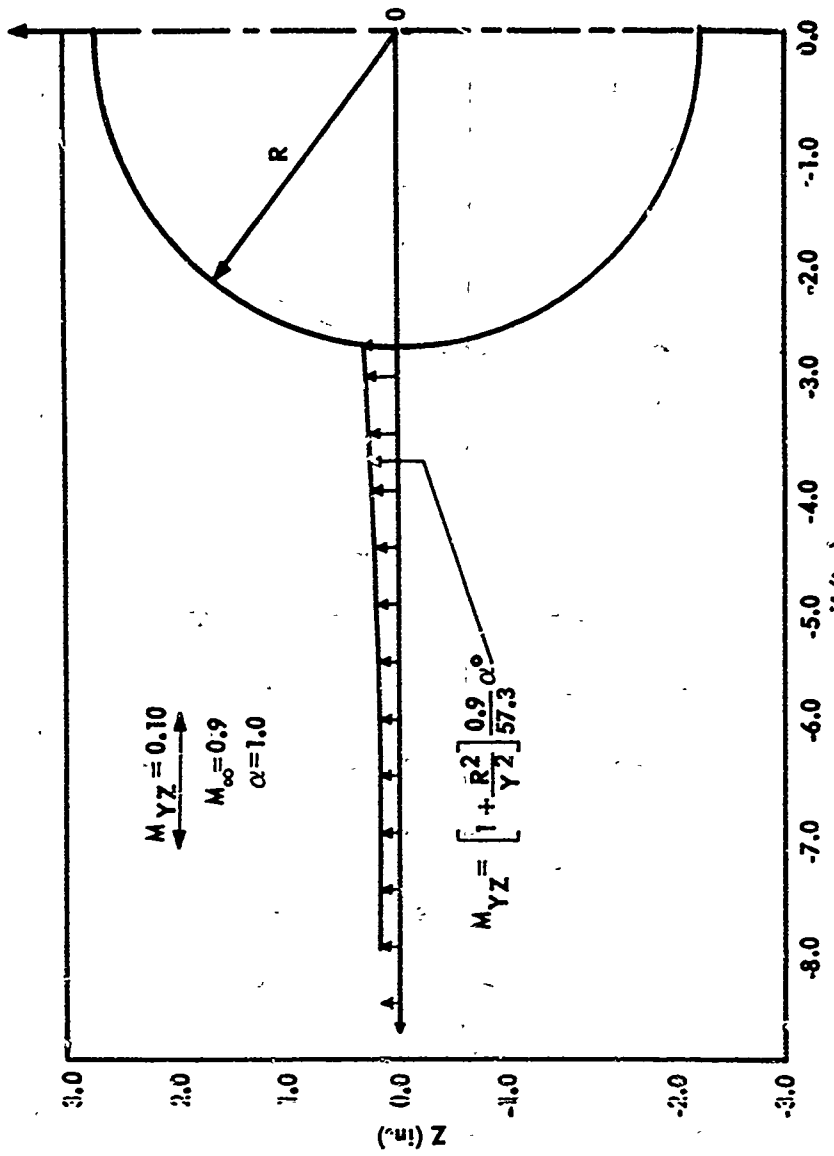

FIGURE 13. FLOW-FIELD THEORY UPWASH COMPARISONS

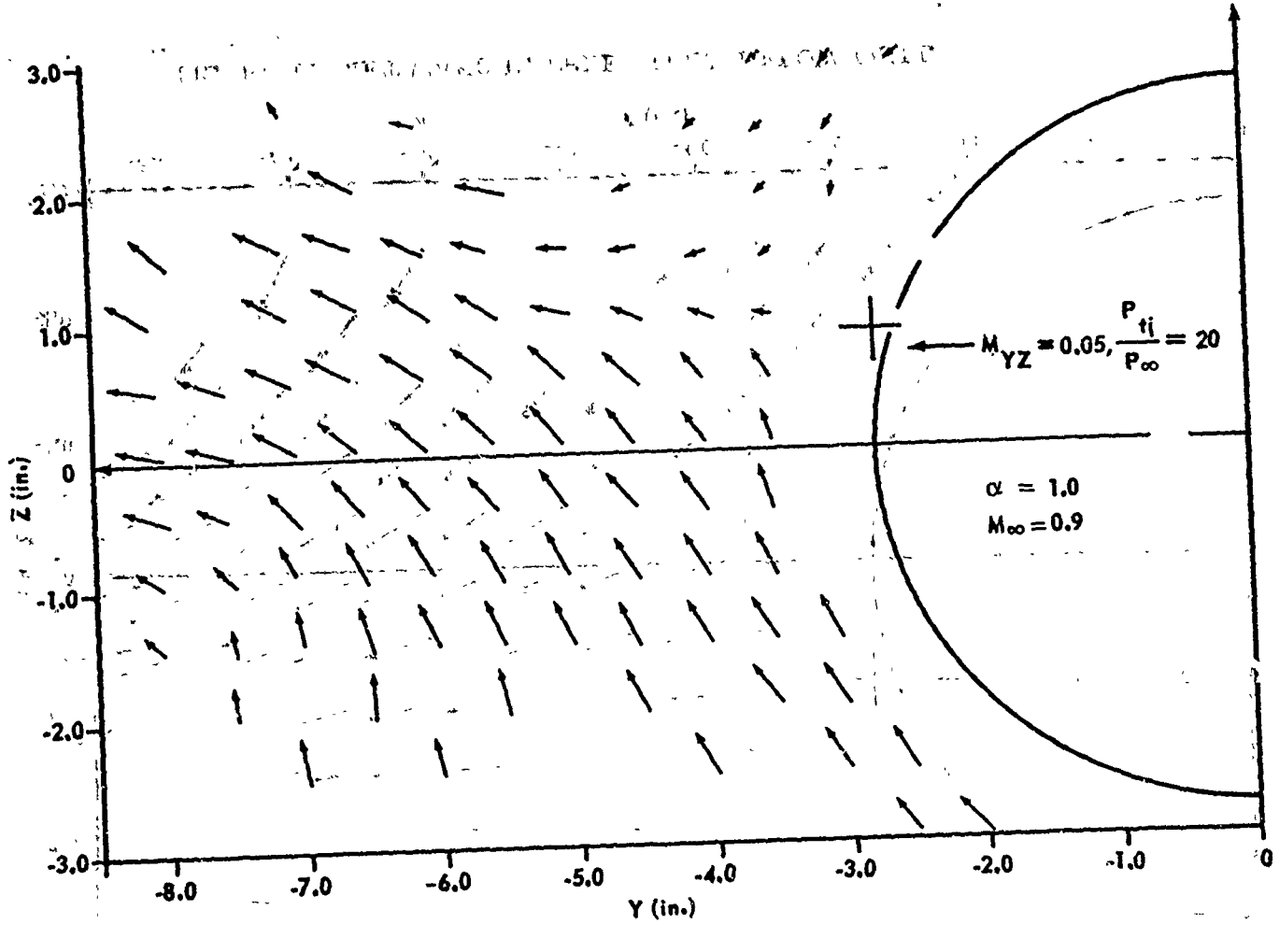

FIGURE 14. JET WAKE IN FREE STREAM FLOW FIELD

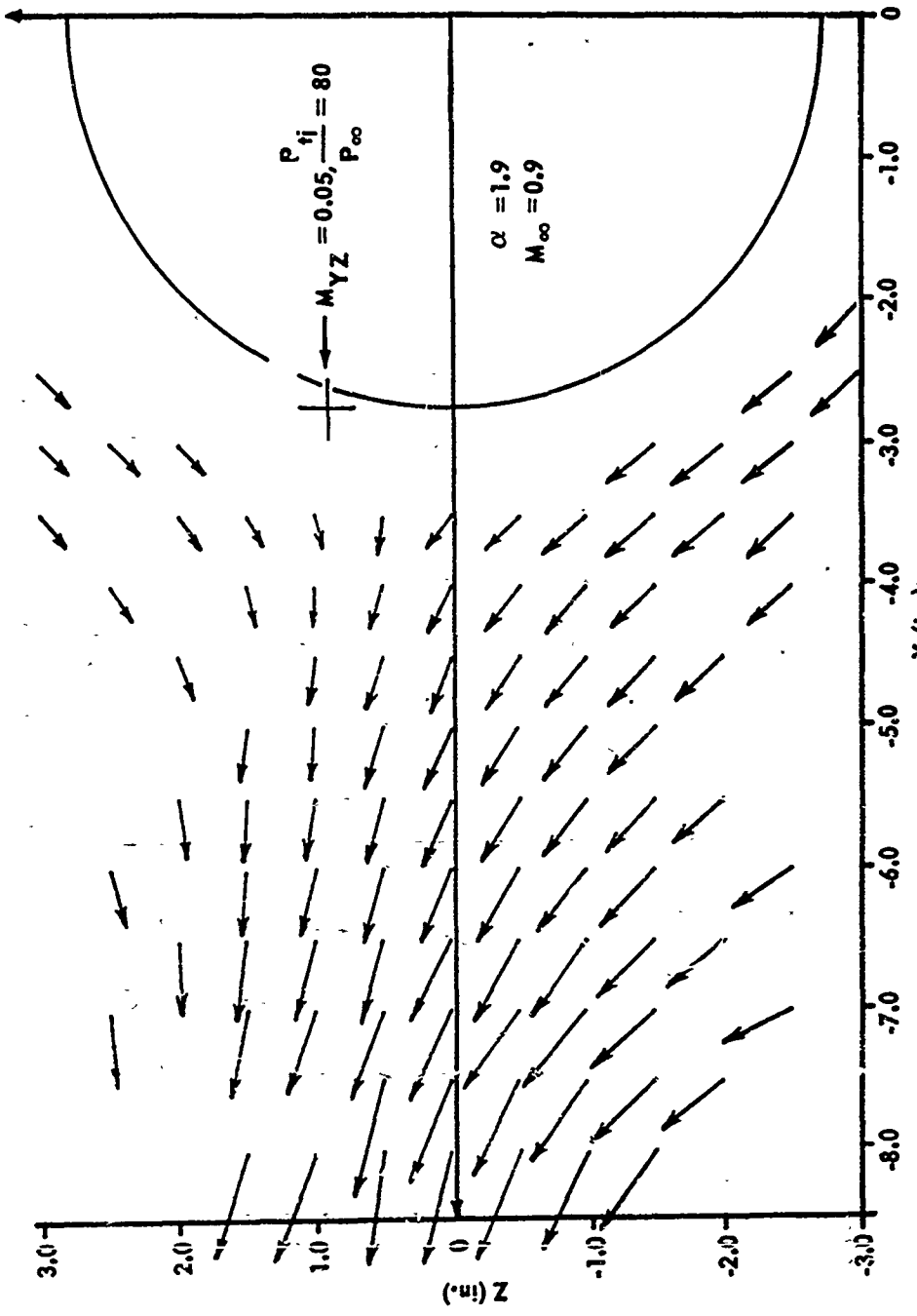

FIGURE 15. JET WAKE IN FREE STREAM FLOW FIELD

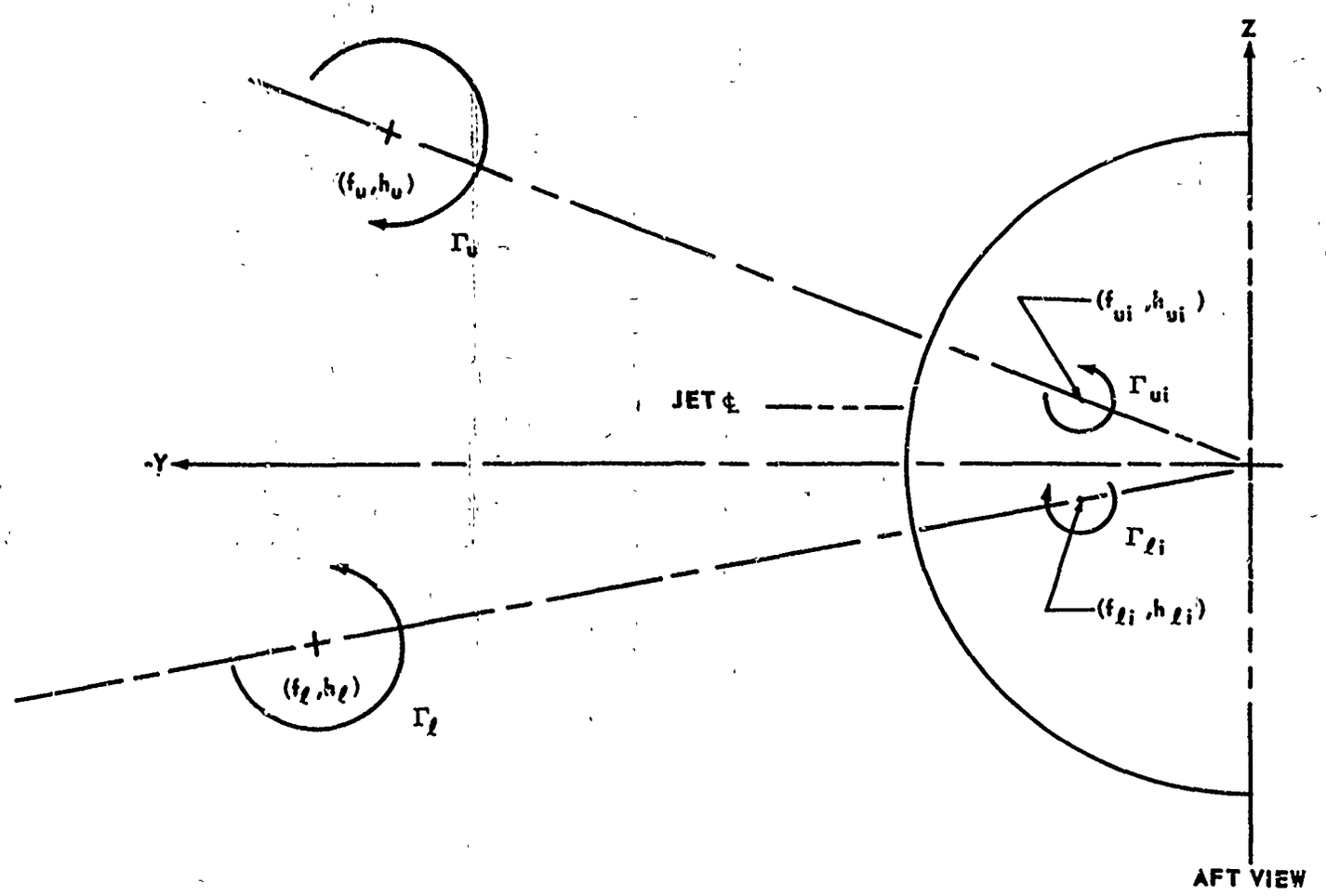

FIGURE 16. VORTEX PATTERN

$$M_Z = \frac{V_Z}{a} = \frac{\Gamma}{a}\frac{1}{2\pi}\left[\frac{Y - f_\ell}{(Y - f_\ell)^2 + (Z - h_\ell)^2} \cdots \frac{Y - f_{\ell i}}{(Y - f_{\ell i})^2 + (Z - h_{\ell i})^2}\right.$$

$$\left. - \frac{Y - f_u}{(Y - f_u)^2 + (Z - h_u)^2} + \frac{Y - f_{ui}}{(Y - f_{ui})^2 + (Y - h_{ui})^2}\right]$$

where

$$f_i = \frac{fR^2}{f^2 + h^2}$$

and

$$h_i = \frac{hR^2}{f^2 + h^2}$$

R = body cylindrical radius.

These relations are known to be deficient in some areas. Two of these areas are:

1) The velocity change in the X direction is not necessarily small compared to velocities in the Y, Z directions.

2) The equations introduce large velocity gradients as the vortex core center is approached, which in real flow, with friction, will be dissapated through viscosity. The viscous core region can be seen on Figure 9.

It appears that these equations give satisfactory comparisons to the flow-field pattern outside of the region of large viscous effects as shown in Figures 17 and 18. If this flow model is proven to be adequate when more experimental data are added, it will lend itself to making force estimates on stabilizing surface. Future tests will be designed toward empirically writing methods for correlating the jet vortex core locations and circulation strength to jet and freestream properties.

5. Conclusions

A wind-tunnel flow-field survey of the downstream wake from a lateral jet located on the forward portion of a body of revolution has led to the following conclusions:

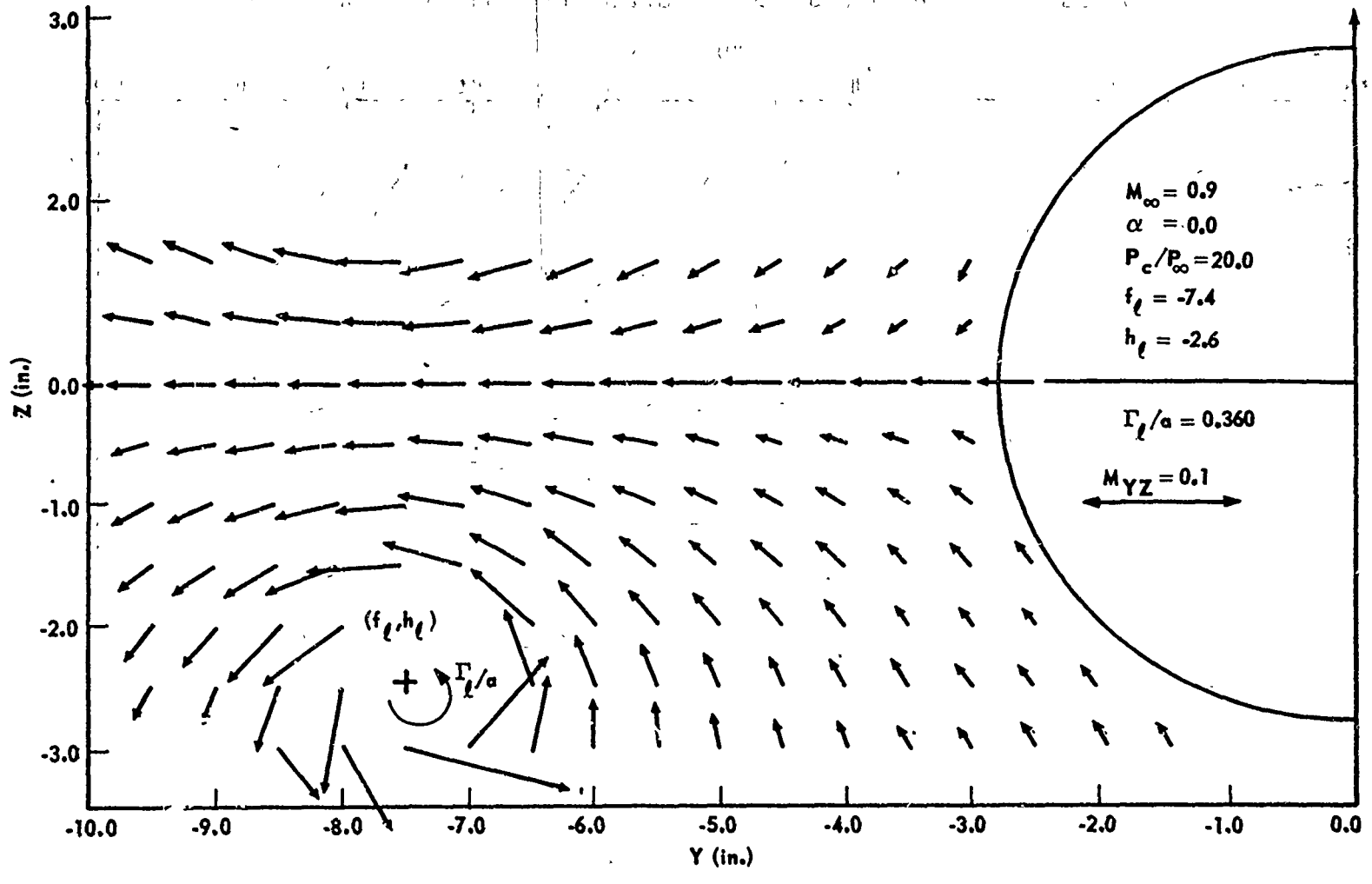

FIGURE 17. COMPUTED FLOW FIELD FROM PLANE VORTEX THEORY

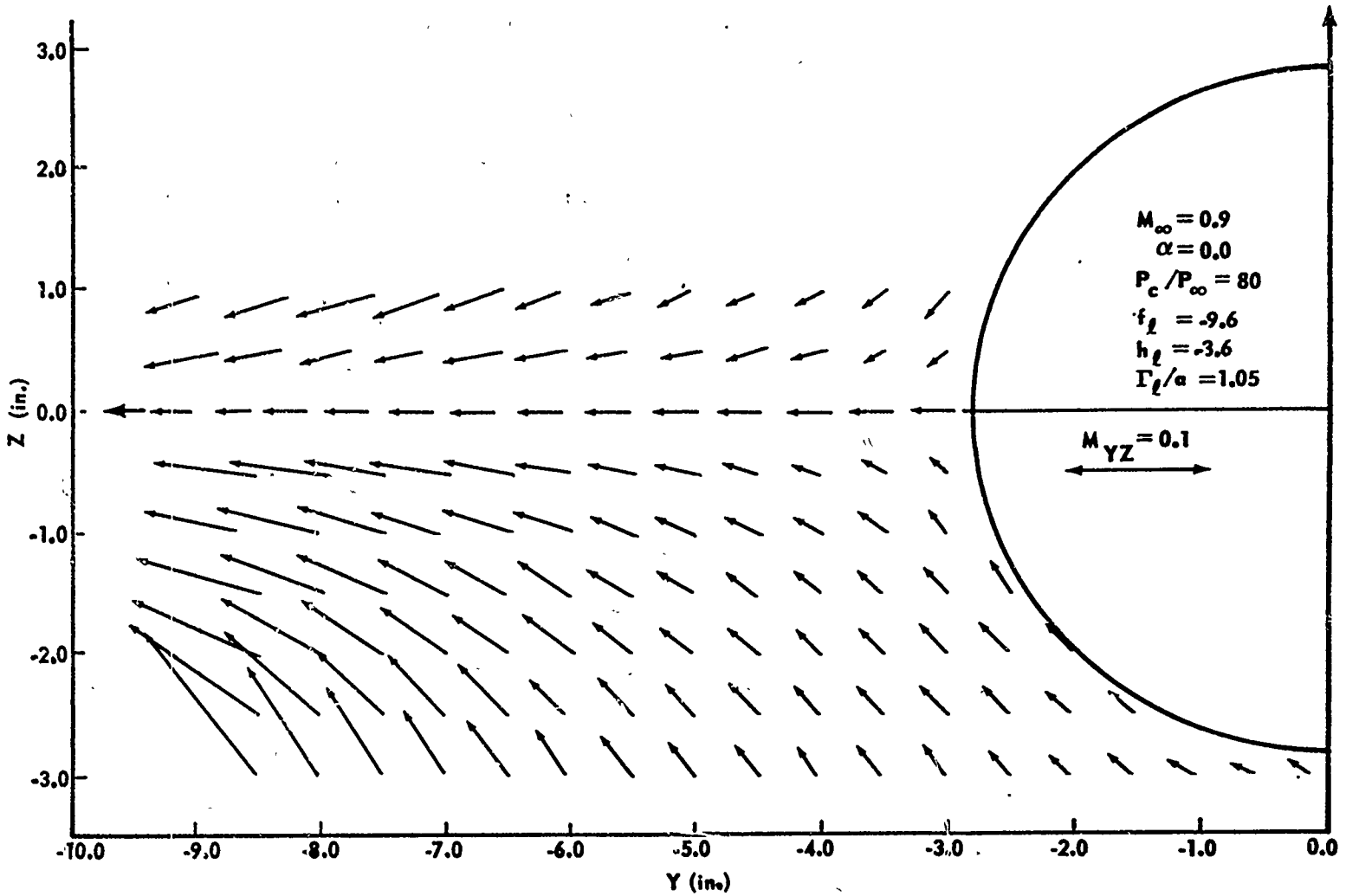

FIGURE 18. COMPUTED FLOW FIELD FROM PLANE VORTEX THEORY

1) This unique means of using a six-hole Pitot-static probe to survey the downstream jet wake in the presence of a body of revolution has proven to be an adequate method of defining the flow-field mechanics.

2) The flow-field model established from results of this test consists of a pair of trailing vortices on opposing sides of the jet centerline, with the vortex centers and vorticity appearing to be primarily functions of jet chamber pressure to freestream static pressure ratio and freestream Mach number.

3) The angle-of-attack case shows a probable shift in the vortex core location or a twisting of the jet wake which hopefully can be related to the cross-flow potential for a body of revolution by combination of the plane vortex and body cross-flow potentials.

4) More efficient planning of future tests of this type can be made through use of these data. Sufficient data of this type can lead to development of mathematical models of the flow field or correlations that can be used to predict the induced forces of the jet wake on stabilizing surface.

LITERATURE CITED

1. Reid, C. F., Jr., The Effects of Several Forward-Mounted Control Jet Nozzles on a Typical Missile Configuration at Transonic Speeds, Cornell Aeronautical Laboratory, Inc., Buffalo, New York, July 1967, Report No. AA-2267-W-3.

2. Dahlke, C. W., Marks, A. S., and Deep, R. A., An Analysis of the Aerodynamic Interaction by Solid Propellant Gas Generator Exhaust for the LANCE Missile (U), U. S. Army Missile Command, Redstone Arsenal, Alabama, July 1966, Report No. RD-TM-66-10 (Confidential).

3. Burt, J. R., Jr., and Dahlke, C. W., Effects of Spin and Vent Tube Jet Flow on LANCE Missile Aerodynamic Coefficients from Analysis of Wind Tunnel Test, LTV Test 246 (U), U. S. Army Missile Command, Redstone Arsenal, Alabama June 1967, Report No. RD-TM-67-4 (Confidential).

4. Dahlke, C. W., A Complete Summary of the Final Aerodynamic Coefficients for All Configurations Flown During the DC-MAW Exploratory Development Program (U), May 1966, Report No. RD-TM-66-8 (Confidential).

5. Spring, D. J., and Martin, T. A., An Experimental Investigation at Transonic Speeds of the Effects of Forward Located Control Jets on the Aerodynamics of the Littlejohn Missile Employing the Thrust Floated Gyro System (U), U. S. Army Missile Command, Redstone Arsenal, Alabama, September 1966, Report No. RD-TM-66-13 (Confidential).

6. Pitts, W. C., Nielsen, J. N., and Kaattari, G. E., Lift and Center of Pressure of Wing-Body-Tail Combinations at Subsonic, Transonic, and Supersonic Speeds, NACA Report 1307, 1959.